



Article scientifique

Article

2024

Published version

Open Access

This is the published version of the publication, made available in accordance with the publisher's policy.

Remote Functionalization by Pd-Catalyzed Isomerization of Alkynyl Alcohols

Scaringi, Simone; Leforestier, Baptiste; Mazet, Clement

How to cite

SCARINGI, Simone, LEFORESTIER, Baptiste, MAZET, Clement. Remote Functionalization by Pd-Catalyzed Isomerization of Alkynyl Alcohols. In: Journal of the American Chemical Society, 2024, vol. 146, n° 27, p. 18606–18615. doi: 10.1021/jacs.4c05136

This publication URL: <https://archive-ouverte.unige.ch/unige:184258>

Publication DOI: [10.1021/jacs.4c05136](https://doi.org/10.1021/jacs.4c05136)

Remote Functionalization by Pd-Catalyzed Isomerization of Alkynyl Alcohols

Simone Scaringi,[†] Baptiste Leforestier,[†] and Clément Mazet*

Cite This: *J. Am. Chem. Soc.* 2024, 146, 18606–18615

Read Online

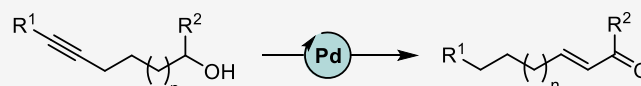
ACCESS |

Metrics & More

Article Recommendations

Supporting Information

ABSTRACT: In recent years, progress has been made in the development of catalytic methods that allow remote functionalizations based on alkene isomerization. In contrast, protocols based on alkyne isomerization are comparatively rare. Herein, we report a general Pd-catalyzed long-range isomerization of alkynyl alcohols. Starting from aryl-, heteroaryl-, or alkyl-substituted precursors, the optimized system provides access preferentially to the thermodynamically more stable α,β -unsaturated aldehydes and is compatible with potentially sensitive functional groups. We showed that the migration of both π -components of the carbon–carbon triple bond can be sustained over several methylene units. Computational investigations served to shed light on the key elementary steps responsible for the reactivity and selectivity. These include an unorthodox phosphine-assisted deprotonation rather than a more conventional β -hydride elimination in the final tautomerization event.



- >25 examples
- moderate to high yield
- high stereocontrol
- long range
- functional group tolerance
- mechanistic study

INTRODUCTION

The field of transition-metal-catalyzed remote functionalizations has grown at an exponential pace over the past decade.¹ In these relay reactions, two distant functional groups can be interconverted by exploiting the reactivity of one function to induce a reaction on the other via a dynamic transmission process, which occurs typically by alkene migration through a hydrocarbon linker (a process referred to as “chain-walking”). With a few exceptions,² the current catalytic methods are based on the formation of the thermodynamically most stable product or the most stable organometallic intermediate, before it is intercepted by an appropriate reagent to install a novel functional group.

In contrast to alkenes, the (long-range) isomerization of alkynes has not witnessed the same level of development. Upon isomerization, the integrity of a C≡C bond can be preserved by migration of the two mutually orthogonal π systems (“alkyne isomerization”; Figure 1, I → II and II → I). Mechanistically, the formation of a transient allene intermediate is generally invoked to account for such processes.^{3,4} Perhaps counterintuitively, the contra-thermodynamic isomerization of internal alkynes to terminal alkynes (often referred to as “alkyne zipper”) has been studied in detail and implemented in the synthesis of several complex structures (Figure 1A, isomerization “out”).^{4,5} A particularly attractive feature of alkyne zipper reactions is their ability to sustain migration over long distances. Nonetheless, the strongly basic conditions employed severely limit functional group tolerance and impose to apply the method at early stages of multistep syntheses or necessitate additional protection/deprotection sequences. Although thermodynamically favored and usually high yielding, the isomerization of terminal alkynes into internal alkynes has received only limited attention,

presumably because the use of a superstoichiometric amount of a strong alkali base is required (Figure 1B, isomerization “in”).⁶ To date, only relocations of the triple bond by one carbon unit have been described. Alkynes can also be isomerized into thermodynamically more stable conjugated 1,3-dienes (Figure 1C; “yne-to-diene” isomerization, I → III). Even though examples of base and phosphine catalysis have been reported, most of the methods developed rely on the use of late transition metals.⁷ In this context, the isomerization of a C≡C bond driven by the conjugation of the diene to an electron-withdrawing substituent is the most documented strategy. The Trost and Lu groups concurrently disclosed highly stereoselective Pd-, Ru-, and Ir-based systems for the isomerization of α,β -ynones, α,β -ynoic esters, and α,β -ynoic amides to the corresponding $\alpha,\beta,\gamma,\delta$ -unsaturated carbonyl derivatives.^{8,9} In comparison, Yamamoto and Hayashi independently established that complex stereoisomeric mixtures are usually obtained in the absence of a stabilizing functional group.^{10,11} More recently, Zhang and co-workers showed that aryl-alkynes and sulfonyl-protected ynamides underwent yne-to-diene isomerization with high levels of stereocontrol under gold catalysis in the presence of an elaborated Buchwald-type monophosphine ligand.¹² While the ruthenium systems employed by Ikawa for the isomerization of propargyl (silyl)ethers and propargyl ethers delivered

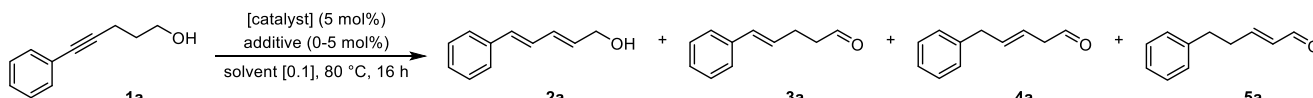
Received: April 15, 2024

Revised: May 31, 2024

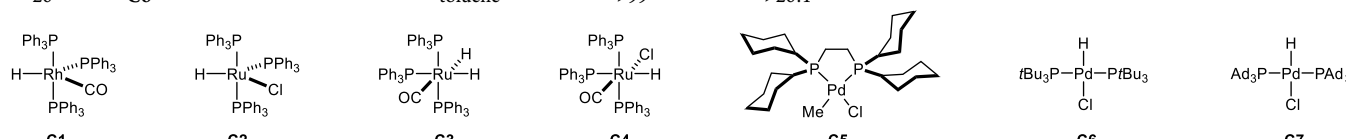
Accepted: June 5, 2024

Published: June 28, 2024



Table 1. Reaction Optimization^a


entry	catalyst/additive	solvent	conv. 2a (%) ^b	(<i>EE</i> / <i>EZ</i>) 2a ^b	conv. 3a + 4a (%) ^{b,c}	conv. 5a (%) ^b	(<i>E</i> / <i>Z</i>) 5a ^b
1	C1	toluene	<5	nd			
2	C2	toluene	<5	nd			
3	C3	toluene	<5	nd			
4	C4	toluene	<5	nd			
5 ^d	C5/NaBAR ^F	toluene	<5	nd			
6	[(Cy ₃ P) ₂ Pd]	toluene	<5	nd			
7	[(<i>t</i> Bu ₃ P) ₂ Pd]	toluene	<5	nd			
8	[(<i>t</i> Bu ₃ P) ₂ Pd]/TsOH	toluene	9	>20:1	~5	<5	nd
9	[(<i>t</i> Bu ₃ P) ₂ Pd]/C ₆ H ₅ CO ₂ H	toluene	12	>20:1	~5	<5	nd
10	[(<i>t</i> Bu ₃ P) ₂ Pd]/(EtO) ₂ P(O)OH	toluene	32	>20:1	~5	<5	nd
11	[(<i>t</i> Bu ₃ P) ₂ Pd]/HBAR ^F	toluene	55	>20:1	~5	<5	nd
12	[(<i>t</i> Bu ₃ P) ₂ Pd]/HCl	toluene	10	9:1	~5	66	>20:1
13	[(Cy ₃ P) ₂ Pd]/HCl	toluene	<5	nd			
14 ^e	C6	toluene	6	9:1	~5	77	>20:1
15 ^e	C7	toluene	14	>20:1	~11	65	>20:1
16 ^e	C6/NaBAR ^F	toluene	48	9:1	~5	34	>20:1
17 ^e	C6	1,2-DCE	5	7:1	15	68	>20:1
18 ^e	C6	2-MeTHF	17	9:1	~5	66	>20:1
19 ^e	C6	CH ₃ CN	70	7:1	~5	16	>20:1
20 ^{e,f}	C6	toluene	>99	>20:1			



^aReactions performed on a 0.05 mmol scale. ^bConversion, stereoselectivity, and stereoisomeric ratio determined by ¹H NMR spectroscopy using an internal standard. ^cComplex stereoisomeric mixture. ^d50 mol % cyclohexene. ^e1 h. ^f25 °C.

(C1–C5) that are effective for the long-range isomerization of C=C bonds (Table 1). In our series of exploratory experiments, no reactivity was observed using the commercially available rhodium and ruthenium hydrides C1–C4 (Table 1, entries 1–4), our homemade biphosphine palladium precatalyst C5 (Table 1, entry 5), or the common palladium precursors [(Cy₃P)₂Pd] and [(*t*Bu₃P)₂Pd] (Table 1, entries 6 and 7). With the idea of generating [Pd–H] species in situ, the latter was used in combination with a variety of protic additives (5 mol %). Isomerization of **1a** into 5-phenylpenta-2,4-dienol (**2a**) was observed using benzoic acid, diethylphosphate, *p*-toluenesulfonic acid, and HBAR^F, with conversions ranging from 9% to 55% and with stereoselectivity systematically >20:1 (Table 1, entries 8–11). These reactions were accompanied by the formation of stereoisomeric mixtures of **3a** and **4a**, several hardly distinguishable internal alkenes, and a trace amount of **5a**. Much to our satisfaction, when hydrochloric acid was employed, the desired α,β -unsaturated aldehyde was obtained as the major product (66%, *E/Z* > 20:1) together with a minor amount of **2a**–**4a** (Table 1, entry 12). No reaction was observed when [(Cy₃P)₂Pd] was employed under otherwise identical reaction conditions, underscoring the importance of the ancillary ligand (Table 1, entry 13). We found that the catalytic performances could be improved using the well-defined complex [(*t*Bu₃P)₂Pd(H)(Cl)] (C6) and, after just 1 h at 80 °C, a 77% conversion to **5a** and a nearly perfect level of stereocontrol (*E/Z* > 20:1) were measured (Table 1, entry 14).¹⁸ Even though appreciable catalytic activity was observed with a [Pd–H] precatalyst

supported by larger trialkylphosphine ligands (C7, L = PdAd₃), conversion in **5a** was noticeably lower (Table 1, entry 15).¹⁹ Finally, the use of NaBAR^F as a halide abstractor and a rapid solvent survey did not lead to any better results (Table 1, entries 16–19). Of particular note, when the isomerization reaction was conducted at room temperature with C6, dienyl alcohol **2a** was obtained quantitatively with perfect stereoselectivity (*EE/EZ* > 20:1) (Table 1, entry 20).²⁰

With the conditions described in Table 1, entry 14, we next assessed the generality of the Pd-catalyzed isomerization of alkynyl alcohols (**1**) into α,β -unsaturated carbonyls (**5**) (24 examples, Figure 2). As a preamble, it should be noted that the products of catalysis (**5**) were systematically obtained with an excellent level of stereocontrol (*E/Z* > 20:1) and usually as the major reaction component. Occasionally, the presence of dienyl alcohol (**2**) or other regioisomers (**3**, **4**, and other internal olefins) rendered purification delicate and affected the yield of pure isolated material. Therefore, to reflect catalytic efficiency, the regioisomeric ratio (*rr*) between **5** and all other (stereo)isomers is indicated in Figure 2. First, we evaluated a series of aryl-substituted substrates where the distance between the C≡C bond and the alcohol functionality was set to three carbon atoms (Figure 2A). We found that the reaction of our model substrate (**1a**) could be conducted on a gram scale without any loss of catalytic efficiency and **5a** was isolated in 61% yield. The use of a secondary alcohol led to a substantially diminished yield and afforded the corresponding α,β -unsaturated ketone **5b** in 33% yield. The introduction of electron-donating substituents in

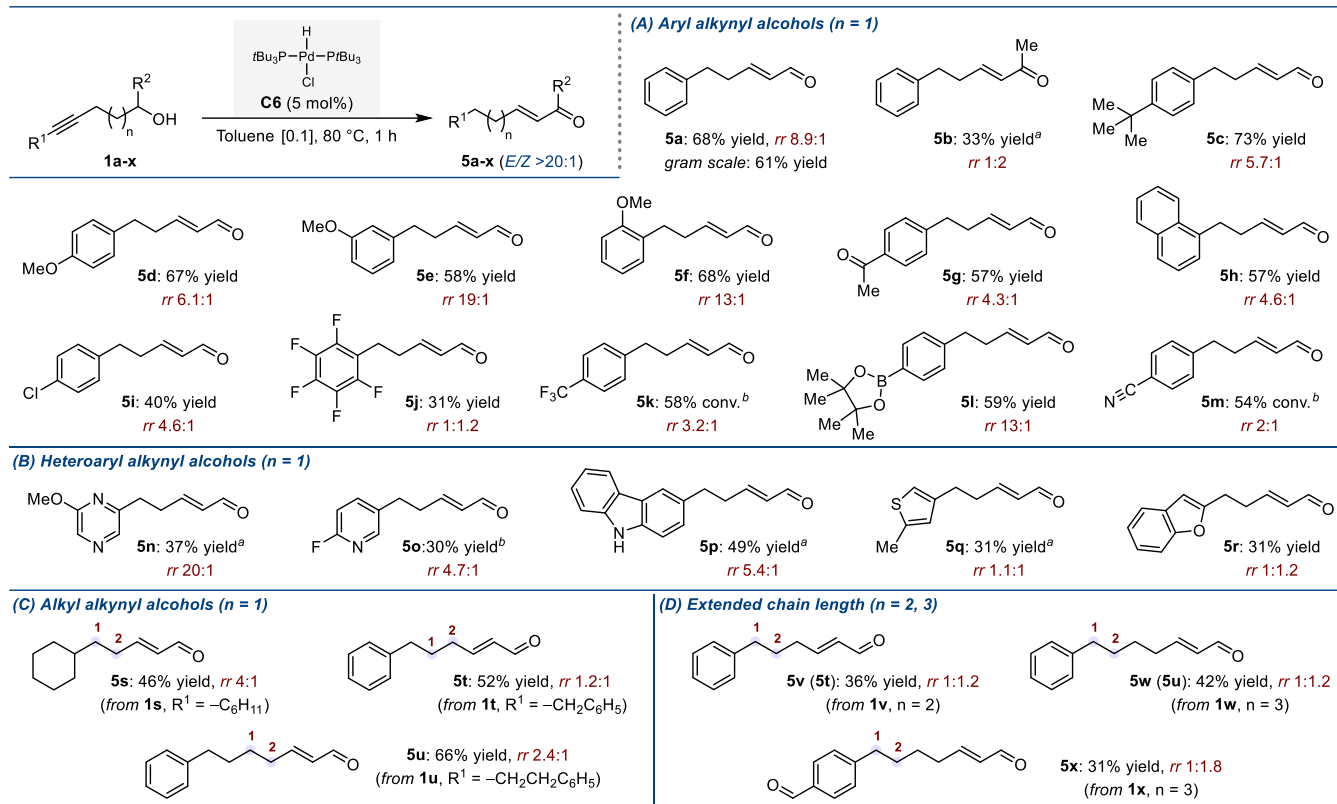


Figure 2. Scope of the Pd-catalyzed isomerization of alkynes into α,β -unsaturated carbonyls. Reaction scale: 0.5 mmol. All products were obtained with $E/Z > 20:1$. Regioisomeric ratio (*rr*) measured by ^1H NMR of the crude reaction mixture using an internal standard and expressed as the ratio between 5 and all other isomers. (A) Isomerization of aryl alkynyl alcohols. (B) Isomerization of heteroaryl alkynyl alcohols. (C) Isomerization of alkyl alkynyl alcohols. (D) Isomerization with extended chain length. ^a3 h. ^bIsolated together with other regioisomers.

the *para*-, *meta*-, and *ortho*-positions was well-tolerated (5c–5f) as was the presence of an enolizable methyl ketone (5g) or a 1-naphthyl group (5h). A reduced catalytic activity was observed for the *p*-chloro (5i), pentafluoroaryl (5j), and *p*-trifluoromethyl (5k) derivatives. Pleasingly, sensitive functional groups such as a boronic ester (5l) and a nitrile (5m) were found to be compatible with the catalytic process. Even though the yields were diminished, we were pleased to find that pyrazine-, pyridine-, and unprotected carbazole-containing substrates were isomerized to the desired α,β -unsaturated aldehydes (5n–5p). Similar results were obtained with a thiophene and a benzofuran derivative (5q–5r) (Figure 2B). The evaluation of alkyl-substituted alkynyl alcohols proved particularly instructive, and the product of remote functionalization was generated preferentially in all cases. While side-products containing an endocyclic double bond were detected using 1s, no sign of styrenyl derivatives were observed with the benzyl- and phenethyl-containing substrates 1t and 1u, suggesting that the formation of the α,β -unsaturated carbonyl is a stronger driving force (Figure 2C). Most notably, we showed that the length of the hydrocarbon chain between the $\text{C}\equiv\text{C}$ bond and the alcohol functionality could be extended up to 5 carbon atoms, although this led to slightly reduced catalytic performances (5v–5x). Attempts to improve these results by re-evaluating standard reaction parameters were not met with success.

Preliminary mechanistic insights were next gleaned experimentally (Figure 3). Resonances attributed to allene intermediates were observed during the monitoring of the catalytic experiment by NMR spectroscopy. The difficulty associated with the purification of these complex mixtures

prompted us to independently prepare compound 6w. In the presence of 5 mol % of $[(t\text{Bu}_3\text{P})_2\text{Pd}(\text{H})(\text{Cl})]$ (C6) in toluene- d_8 , conversion of 6w into dienyl alcohol 2w occurred within minutes at room temperature (Figure 3A). Next, placing the same sample at 80 °C led after 3 h to the formation of the α,β -unsaturated aldehyde 5w (46% conv., $E/Z > 20:1$) along with ca. 12% of internal olefins. These experiments support the notion that both allenes and dienyl alcohols are intermediates in the long-range Pd-catalyzed isomerization of alkynyl alcohols and that the process is likely to proceed by iterative migratory insertion/ β -hydride elimination sequences.²¹ When the α,β -unsaturated aldehyde 5a was resubjected to catalysis, no reaction occurred. In contrast, related ketone 5b was partially converted into styrenyl 3b (Figure 3B). Retrospectively, these results explain the reduced yield obtained in the isomerization of the alkynyl secondary alcohol 1b. More importantly, they indicate that α,β -unsaturated ketones are susceptible to be deconjugated, while isomerization of primary alkynyl alcohols is not reversible under the optimized reaction conditions. Finally, isomerization of the enantioenriched substrate (*R*)-1y (97:3 *er*) yielded a 4:1 mixture of dienyl alcohol 2y and α,β -unsaturated aldehyde 5y, albeit in racemic form. This not only indicates that isomerization toward the α,β -unsaturated aldehyde is not completely interrupted by the presence of an alkyl substituent on the hydrocarbon chain but it also implies that the catalyst dissociates during the migration of the two π components of the initial alkyne.²² When the alkynyl methyl ether derivative 1w.Me was subjected to the optimized reaction conditions, after 1 h, formation of diene 2w.Me was observed along with a complex mixture of alkenes in a ca. 2:1 ratio (Figure 3D). Prolonging the

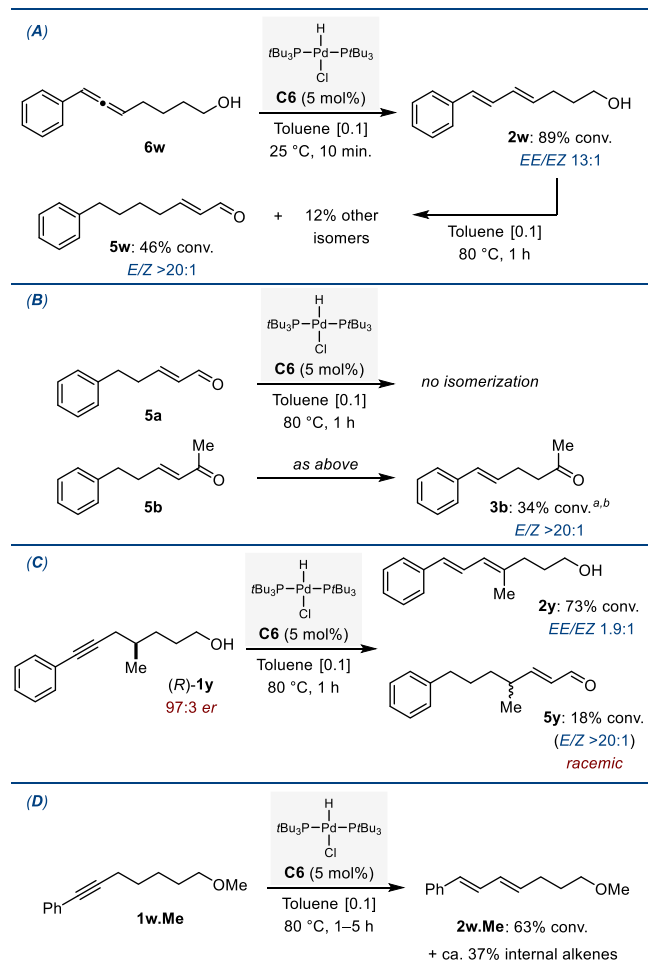


Figure 3. (A) Isomerization of allene **6w**. (B) Evaluation of the reversibility of the catalytic reaction. (C) Isomerization of an enantioenriched substrate. (D) Isomerization of alkynyl methyl ether **1w.Me**. ^aContains ca. 5% of **4b**. ^bConversion reaches 37% after 3 and 5 h.

reaction time to 3 or even 5 h did not change the outcome of the reaction significantly, suggesting that a thermodynamic equilibrium has been reached. This result indicates that although the hydroxyl functionality is not required to trigger the first elementary steps, it is a necessary thermodynamic driving force for the formation of α,β -unsaturated aldehydes.

To obtain additional information on the thermodynamic parameters of the reaction, a computational study based on density functional theory (DFT) combined with post-Hartree–Fock methods was conducted using the ORCA 5.0.4 software package.²⁴ The relative stabilities of **1a** (thereafter denoted as **SM**_{1–1}) and its most relevant (stereo)isomers intervening in the isomerization process to **5a** (thereafter denoted as **P**_{3–5}) are displayed in Figure 4. While initial conversion of the alkyne to the parent allene (**Int**_{1–2}) does not result in any thermodynamic stabilization, further migration of the π system to afford conjugated diene **Int**_{1–3} constitutes a first thermodynamic sink, which lowers the energy of the system by 13.5 kcal/mol. Further delocalization to afford skipped diene **Int**_{1–4} or conjugated dienol **Int**_{2–4} is essentially isoenergetic (–12.8 and –14.9 kcal/mol, respectively). By contrast, all of the computed aldehydes benefit from an additional stabilization energy of ca. 10 kcal/mol when compared to their enol precursors, whereby the final α,β -unsaturated aldehyde (**P**_{3–5}) is calculated to be the

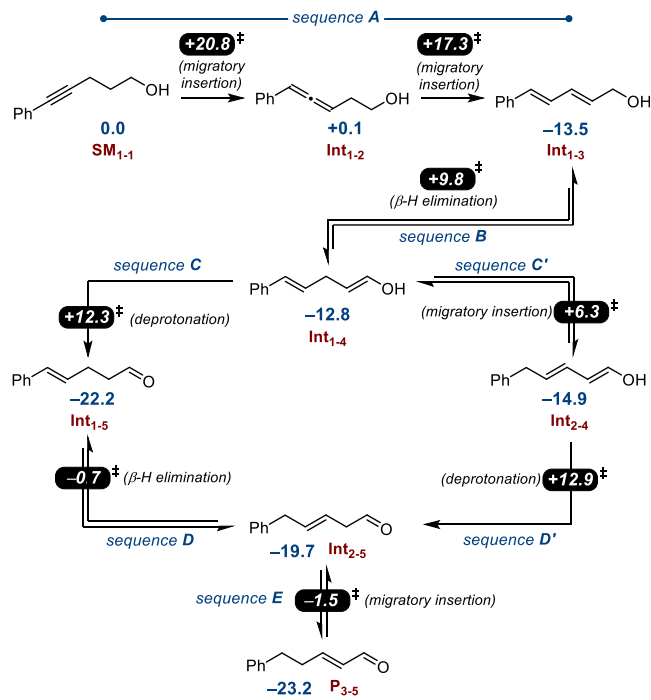


Figure 4. Free energy (kcal/mol) of intermediates along the isomerization pathway relative to substrate **1a/SM**_{1–1}. Calculated at the DLPNO-CCSD(T)/def2-TZVPP// ω B97X-D3(BJ)/def2-mTZVPP level of theory with CPCM (toluene). Black boxes along the arrows indicate the highest-energy transition state between the linked intermediates in the isomerization sequence, with reference to **SM**_{1–1} and **C6**. The nature of said transition state is indicated in parentheses.²³

most thermodynamically stable compound (sequence C \rightarrow sequence D \rightarrow sequence E). This is in full agreement with our experimental observations. Our calculations were also in line with the deconjugative isomerization of ketone **5b** into **3b** when subjected to the catalytic conditions (Figure 3B and Section S6.8). Indeed, a $\Delta\Delta G$ of 0.8 kcal/mol was calculated in favor of the styrenyl derivative compared to the α,β -unsaturated ketone. Collectively, these results suggest a degree of reversibility in the isomerization processes occurring between the various aldehydes leading to a thermodynamic mixture.

The entire mechanism of the Pd-catalyzed isomerization of alkynyl alcohol **SM**_{1–1} was explored next. Sequence A leading to diene **Int**_{1–3} is presented in detail in Figure 5. We found that displacement of a phosphine ligand and binding of the substrate lead to complex **A.1** with an energy penalty calculated at +15.9 kcal/mol. Migratory insertion of the alkyne occurs via **TS**_{A.1–2}, which lies at +20.8 kcal/mol. Subsequent β -hydride elimination from **A.2** was calculated to be relatively facile (+19.3 kcal/mol) and yields the π -bound allene (**A.3**). Likewise, further migratory insertion proceeds with a low barrier (+17.3 kcal/mol) to furnish *anti/syn* π -allyl palladium complex **A.4**. Because this intermediate lies at –10.3 kcal/mol on the pathway from its parent transition state **TS**_{A.3–4}, its formation is likely to be irreversible and therefore prevents forming back either the allene (**Int**_{1–2}) or the alkyne (**SM**_{1–1}). From **A.4**, a π – σ – π isomerization sequence results in *anti*–*syn* interconversion of the phenyl substituent by rotation around the σ (C–C) bond in the η^1 -Pd-benzyl intermediates **A.5** and **A.6** to finally generate the *syn/syn* π -allyl palladium **A.7** (with an associated activation energy of $\Delta G^\ddagger = 16.2$ kcal/mol).

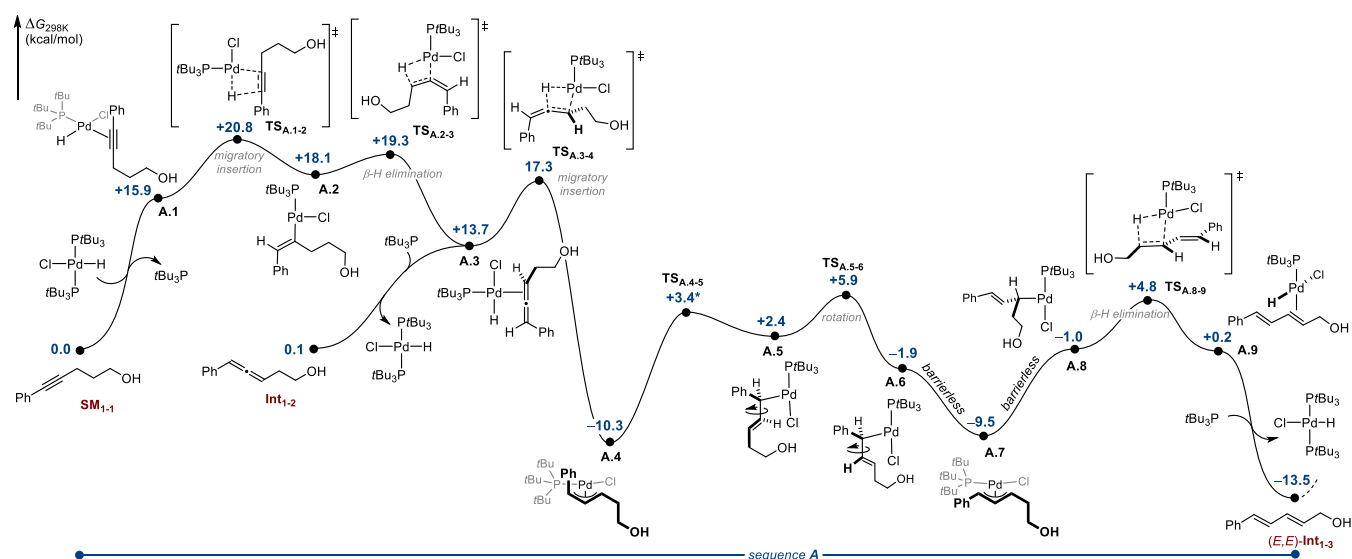


Figure 5. Computed free-energy profile for sequence A of the Pd-catalyzed isomerization of alkynyl alcohol **1a**/**SM**₁₋₁. Level of theory: DLPNO-CCSD(T)/def2-TZVPP// ω B97X-D3(BJ)/def2-mTZVPP with CPCM(toluene). * $TS_{A,4-5}$ was located as the climbing image of a nudged elastic band (NEB-CI) calculation.²³

The only path forward to **Int**₁₋₃ we could identify consists of a rapid conversion to energetically accessible σ -allyl palladium intermediate **A.8**, which can engage in a subsequent β -hydride elimination with the adjacent methylene unit through a transition state located at +4.8 kcal/mol ($TS_{A,8-9}$). Overall, with the highest barrier calculated at $\Delta G^\ddagger = +20.8$ kcal/mol for the migratory insertion of the [Pd-H] across the alkyne moiety, our calculations suggest that the allene **Int**₁₋₂ (although an intermediate) may not be isolable in the presence of the catalytic system. Indeed, rapid conversion to **A.4** is expected even at room temperature. This result is fully consistent with the conversion of allene **6w** into **2w** at room temperature within minutes, as observed experimentally. Moreover, with an activation barrier to revert to **A.7** lying at $\Delta G^\ddagger = 18.3$ kcal/mol, the formation of **Int**₁₋₃ is likely reversible. Even though they were found to be thermodynamically slightly less stable, all other stereoisomers of (*E,E*)-**Int**₁₋₃ are theoretically accessible at room temperature (see Section S6.9). Conversion of the conjugated diene **Int**₁₋₃ into the skipped diene **Int**₁₋₄ is accomplished through consecutive migratory insertion ($TS_{B,1-2}$) and β -hydride elimination ($TS_{B,2-3}$) via the intermediacy of the agostic complex **B.2** (sequence B, Figure 6). The overall barrier of $\Delta G^\ddagger = 23.3$ kcal/mol in sequence B is higher than that in sequence A. This is consistent with the possibility to isolate dienyl alcohol **2**. While no transition state could be successfully optimized between **A.9** and **Int**₁₋₃ (Figure 5), the accumulation of the latter at room temperature before further isomerization to **Int**₁₋₄ suggests that decooordination is facile. This hypothesis is in line with the results disclosed in Figure 3C (vide supra). From pivotal intermediate **Int**₁₋₄, conversion into **Int**₂₋₄ is energetically facile ($\Delta G^\ddagger = 19.1$ kcal/mol). Of note, this relatively stable dienol lying at -14.9 kcal/mol may act as a temporary reservoir before tautomerization into **Int**₂₋₅ or may convert back to **Int**₁₋₄, which subsequently tautomerizes into **Int**₁₋₅. Retrospectively, **Int**₁₋₄ and **Int**₂₋₄ (and stereoisomers thereof) may likely be the various internal alkenes observed experimentally (vide supra). To access the next pivotal intermediate (**Int**₂₋₅, lying at -19.7 kcal/mol), sequences C \rightarrow D and C' \rightarrow D' are equally energetically viable and exhibit similar idiosyncrasies.

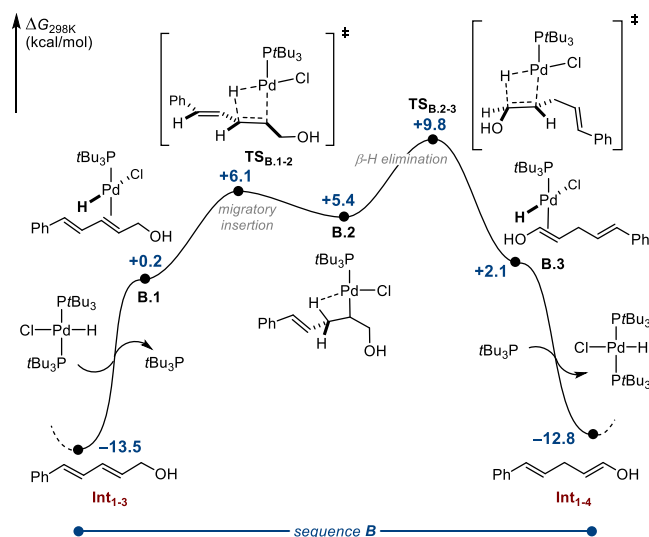


Figure 6. Computed free-energy profile for sequence B of the Pd-catalyzed isomerization of alkynyl alcohol **1a**/**SM**₁₋₁. Level of theory: DLPNO-CCSD(T)/def2-TZVPP// ω B97X-D3(BJ)/def2-mTZVPP with CPCM(toluene).²³

Therefore, for the sake of brevity, in the following section, we will only discuss the nature of the intermediates intervening in the slightly favored sequence C \rightarrow D. The full free-energy profiles of sequences C' and D' are available in the Supporting Information.

Tautomerization of **Int**₁₋₄ into **Int**₁₋₅ presents some unorthodox features (sequence C, Figure 7). Coordination to the enol followed by migratory insertion is endergonic and occurs with an overall barrier of $\Delta G^\ddagger = 22.6$ kcal/mol. Generation of **Int**₁₋₅ via a conventional β -hydride elimination from agostic palladium complex **C.2** was found to be kinetically inaccessible for our system ($TS_{C,3-Int1-5}$ lies at +27.8 kcal/mol). Instead, a transition state involving the spare equivalent of *t*Bu₃P acting as a base to deprotonate the alcohol proved to be more favorable and constitutes a potential rate-determining step with TS_{C4-5} at +12.3 kcal/mol. Calculated from **Int**₂₋₄, this leads to

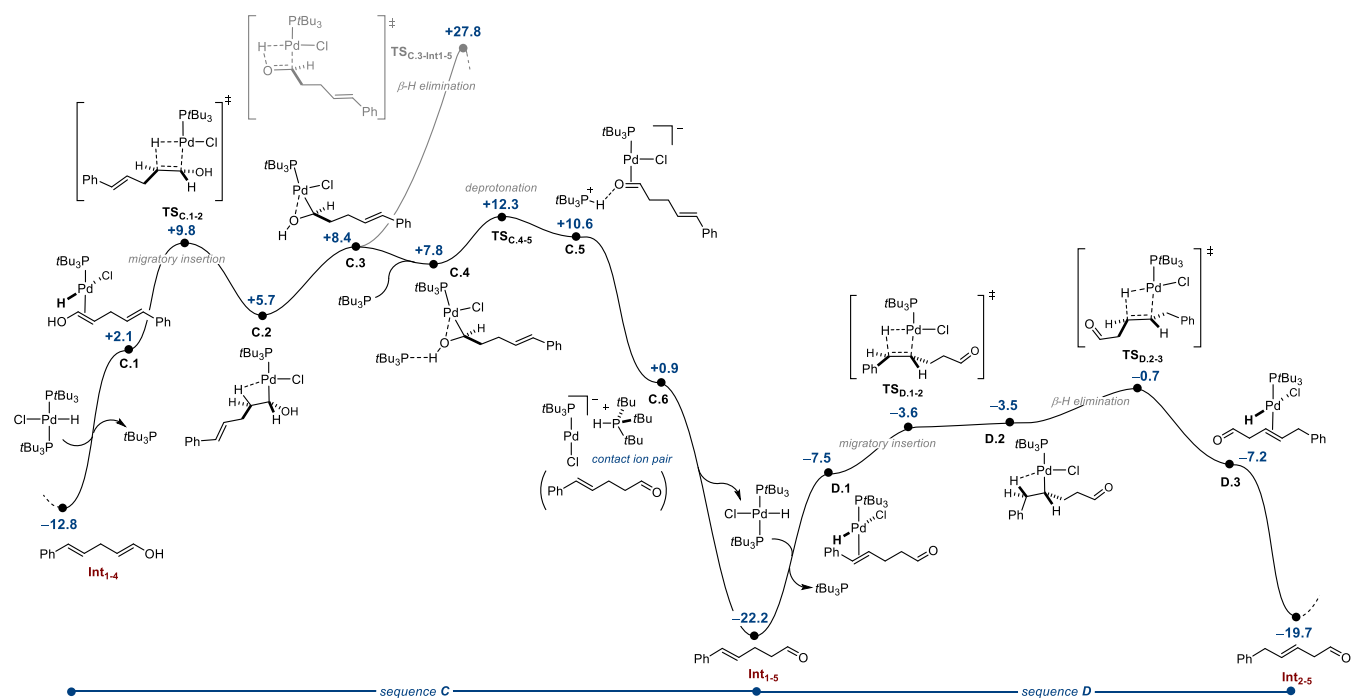


Figure 7. Computed free-energy profile for sequences C and D of the Pd-catalyzed isomerization of alkynyl alcohol **1a**/ SM_{1-1} . Level of theory: DLPNO-CCSD(T)/def2-TZVPP// ω B97X-D3(BJ)/def2-mTZVPP with CPCM(toluene).²³

an overall activation barrier for the full isomerization process estimated at $\Delta G^\ddagger = 27.2$ kcal/mol, which is consistent with the elevated temperatures needed to promote complete isomerization. Of important note, keto–enol tautomerization involving [Pd–H] intermediates has previously been suggested to involve DMF as a proton shuttle.²⁵ Toluene, the solvent used in our optimized catalytic conditions, does not offer such proton-shuttling capability. Similarly, a non-catalyzed tautomerization via a dimeric pathway was previously calculated to be kinetically unrealistic.^{22c} Even though we are well within the expected accuracy compared to experimental data, TS_{C4-5} might be slightly overestimated due to possible limitations of implicit solvent models for charged separated species.²⁶ The π -bound carbonyl intermediate resulting from proton abstraction (C.5) is formally a negatively charged Pd(0) complex hydrogen-bonded to the phosphonium salt. This species subsequently evolves into a tight-contact ion pair (C.6) before the release of Int_{1-5} and regeneration of precatalyst [(tBu₃P)₂Pd(H)(Cl)]. Sequence D, in which Int_{1-5} is converted into Int_{2-5} by deconjugation of the styrenyl unit, is composed of a more conventional sequence of migratory insertion and β -H elimination, the latter presenting the highest barrier at -0.7 kcal ($\Delta G^\ddagger = 21.5$ kcal/mol from Int_{1-5}). From Int_{2-5} , conjugation of the C=C bond with the carbonyl to afford the final α,β -unsaturated aldehyde P_{3-5} proceeds again via a migratory insertion/ β -H elimination process (sequence E, Figure 8). The corresponding transition states are located at similar energy levels and are likely to occur rapidly at room temperature with activation energy comprised between 17.9 and 18.2 kcal/mol. Furthermore, the relatively low barriers computed in sequences D and E suggest that thermal equilibration between aldehydes Int_{1-5} , Int_{2-5} , and P_{3-5} is rapid under the optimized reaction conditions. This observation is consistent with the fact that the regioisomeric ratio between these three species is dictated by thermodynamics (note that the predicted ΔG of 1.0 kcal/mol is in relatively good agreement with the regioisomeric ratio measured experimentally for **5a**).²⁷

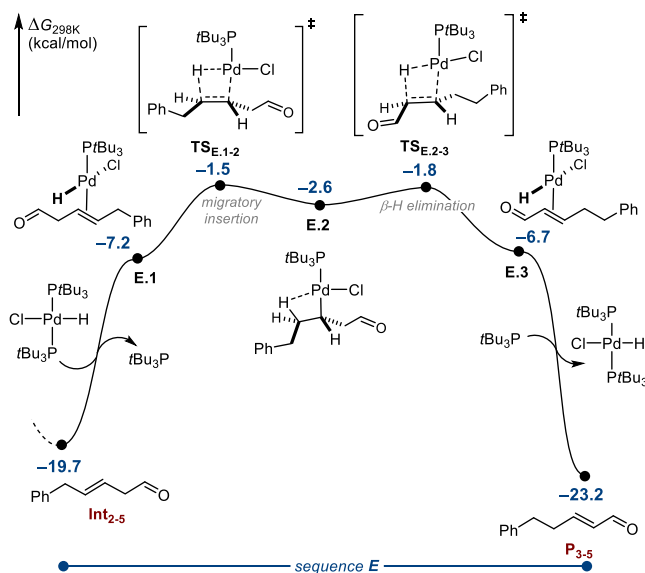


Figure 8. Computed free-energy profile for sequence E of the Pd-catalyzed isomerization of alkynyl alcohol **1a**/ SM_{1-1} . Level of theory: DLPNO-CCSD(T)/def2-TZVPP// ω B97X-D3(BJ)/def2-mTZVPP with CPCM(toluene).²³

Because P_{3-5} is calculated to be the thermodynamic product, the apparent lack of reactivity of **5a** when subjected to catalysis may not result from irreversibility but rather from a thermodynamic equilibrium that lies in favor of the α,β -unsaturated product.

CONCLUSIONS

In summary, using a readily available palladium hydride complex, we developed a catalytic isomerization of alkynyl alcohols. The operationally simple protocol is effective for aryl-, heteroaryl-, and alkyl-containing substrates and provides access preferentially to the thermodynamically more stable α,β -

unsaturated aldehydes in practical yields. We found that the functional group tolerance is broad and that the isomerization of both π -components of the initial $C\equiv C$ bond can be sustained over several methylene units. Computational analyses were in agreement with our preliminary experimental mechanistic investigations. While most elementary steps consist of successive migratory insertion/ β -hydride elimination sequences, we identified an unusual phosphine-assisted deprotonation as being energetically more favorable than a conventional β -hydride elimination in the rate-determining aldehyde-forming tautomerization steps. We anticipate that the results disclosed in our study may broaden the field of remote functionalizations by adding alkynes as a potential entry point in the arsenal of synthetic chemists.

ASSOCIATED CONTENT

Supporting Information

The Supporting Information is available free of charge at <https://pubs.acs.org/doi/10.1021/jacs.4c05136>.

Experimental procedures, characterization of all new compounds, spectroscopic data, and computational procedures (PDF)

Additional data (ZIP)

Molecular coordinates of computed structures (XYZ)

AUTHOR INFORMATION

Corresponding Author

Clément Mazet – Department of Organic Chemistry, University of Geneva, 1211 Geneva, Switzerland; orcid.org/0000-0002-2385-280X; Email: clement.mazet@unige.ch

Authors

Simone Scaringi – Department of Organic Chemistry, University of Geneva, 1211 Geneva, Switzerland

Baptiste Leforestier – Department of Organic Chemistry, University of Geneva, 1211 Geneva, Switzerland; orcid.org/0000-0001-8547-6021

Complete contact information is available at: <https://pubs.acs.org/10.1021/jacs.4c05136>

Author Contributions

[†]S.S. and B.L. contributed equally.

Notes

The authors declare no competing financial interest.

ACKNOWLEDGMENTS

This work was supported by the Swiss National Science Foundation (200021_188490) and the University of Geneva. The authors thank Stéphane Rosset (University of Geneva) for technical assistance and for measuring HRMS. F. Dubler and Dr. J. Rostoll-Berenguer (University of Geneva) are acknowledged for their experimental contributions. Part of the computations were performed at the University of Geneva on the “Yggdrasil” HPC cluster. The authors also thank Dr. Amalia I. Poblador-Bahamonde (University of Geneva) for offering access to her computational facilities.

REFERENCES

- (1) (a) Larionov, E.; Li, H.; Mazet, C. Well-Defined Transition Metal Hydrides in Catalytic Isomerizations. *Chem. Commun.* **2014**, *50*, 9816. (b) Vasseur, A.; Bruffaerts, J.; Marek, I. Remote Functionalization through Alkene Isomerization. *Nat. Chem.* **2016**, *8*, 209. (c) Sommer, H.; Julia-Hernández, F.; Martin, R.; Marek, I. Walking Metals for Remote Functionalization. *ACS Cent. Sci.* **2018**, *4*, 153. (d) Kochi, T.; Kanno, S.; Kakiuchi, F. Nondissociative Chain Walking as a Strategy in Catalytic Organic Synthesis. *Tetrahedron Lett.* **2019**, *60*, No. 150938. (e) Massad, I.; Marek, I. Alkene Isomerization through Allylmetals as a Strategic Tool in Stereoselective Synthesis. *ACS Catal.* **2020**, *10*, 5793. (f) Janssen-Müller, D.; Sahoo, B.; Sun, S.-Z.; Martin, R. Tackling Remote sp^3 C–H Functionalization via Ni–Catalyzed “chain-walking” Reactions. *Isr. J. Chem.* **2020**, *60*, 195. (g) Fiorito, D.; Scaringi, S.; Mazet, C. Transition metal–catalyzed alkene isomerization as an enabling technology in tandem, sequential and domino processes. *Chem. Soc. Rev.* **2021**, *50*, 1391. (h) Ghosh, S.; Patel, S.; Chatterjee, I. Chain-walking reactions of transition metals for remote C–H bond functionalization of olefinic substrates. *Chem. Commun.* **2021**, *57*, 11110.
- (2) For a review, see: (a) Scaringi, S.; Mazet, C. Transition Metal-Catalyzed (Remote) Deconjugative Isomerization of α,β -Unsaturated Carbonyls. *Tetrahedron Lett.* **2022**, *96*, No. 153756. For selected examples using transition metal catalysts, see: (b) Lin, L.; Romano, C.; Mazet, C. Palladium-Catalyzed Long-Range Deconjugative Isomerization of Highly Substituted α,β -Unsaturated Carbonyl Compounds. *J. Am. Chem. Soc.* **2016**, *138*, 10344. (c) Borah, A. J.; Shi, Z.-Z. Rhodium-Catalyzed, Remote Terminal Hydroarylation of Activated Olefins through a Long-Range Deconjugative Isomerization. *J. Am. Chem. Soc.* **2018**, *140*, 6062. (d) Hanna, S.; Butcher, T. W.; Hartwig, J. F. Contrainformational Olefin Isomerization by Chain-Walking Hydrofunctionalization and Formal Retro-hydrofunctionalization. *Org. Lett.* **2019**, *21*, 7129. (e) Li, C.; Zhang, K.; Zhao, W. *ACS Catal.* **2024**, *14*, 5458.
- (3) Avocetien, K.; Li, Y.; O’Doherty, G. A. *The Alkyne Zipper Reaction in Asymmetric Synthesis*; Barry, M.; Trost, C.-J. L., Eds.; Wiley and Sons: Weinheim, Germany, 2014.
- (4) (a) Danilkina, N. A.; Vasileva, A. A.; Balova, I. A. A.E. Favorskii’s scientific legacy in modern organic chemistry: prototropic acetylene – allene isomerization and the acetylene zipper reaction. *Russ. Chem. Rev.* **2020**, *89*, 125. (b) Sørskår, Å. M.; Stenstrøm, H. Ø. K.; Stenstrøm, Y.; Antonsen, S. G.; et al. The Alkyne Zipper Reaction: A Useful Tool in Synthetic Chemistry. *Reactions* **2023**, *4*, 26.
- (5) For selected examples of alkyne zipper in synthesis, see: (a) Kirkham, J. E. D.; Courtney, T. D. L.; Lee, V.; Baldwin, J. E. Asymmetric synthesis of cytotoxic sponge metabolites R-strongyloidiols A and B. *Tetrahedron Lett.* **2004**, *45*, 5645. (b) Hoyer, R. C.; Anderson, G. L.; Brown, S. G.; Schultz, E. E. Total Synthesis of Clathculins A and B. *J. Org. Chem.* **2010**, *75*, 7400. (c) Das, S.; Kuilya, T. K.; Goswami, R. K. Asymmetric Total Synthesis of Bioactive Natural Lipid Mycalol. *J. Org. Chem.* **2015**, *80*, 6467. (d) Avocetien, K. F.; Li, J. J.; Liu, X.; Wang, Y.; Xing, Y.; O’Doherty, G. A. De Novo Asymmetric Synthesis of Phoracantholide. *Org. Lett.* **2016**, *18*, 4970. (e) Xu, F.; Zhong, Y. L.; Li, H. M.; Qi, J.; Desmond, R.; Song, Z. G. J.; Park, J.; Wang, T.; Truppo, M.; Humphrey, G. R.; Ruck, R. T. Asymmetric Synthesis of Functionalized Trans-Cyclopropoxy Building Block for Grazoprevir. *Org. Lett.* **2017**, *19*, 5880.
- (6) (a) Seiichi, T.; Shimazaki, Y.; Iwabuchi, Y.; Ogasawara, K. A convergent enantiocontrolled route to mevalonolactone and vitamin E from (S)-O-benzylglycidol. *Tetrahedron Lett.* **1990**, *31*, 3619. (b) Thompson, C. F.; Jamison, T. F.; Jacobsen, E. N. FR901464: Total Synthesis, Proof of Structure, and Evaluation of Synthetic Analogues. *J. Am. Chem. Soc.* **2001**, *123*, 9974.
- (7) (a) Farmer, M. L.; Billups, W. E.; Greenlee, R. B.; Kurtz, A. N. Isomerization of Propargylic Amines to Conjugated Dienes. 2-Dialkylamino-1,3-butadienes. *J. Org. Chem.* **1966**, *31*, 2885. (b) Trost, B. M.; Kazmaier, U. Internal redox catalyzed by triphenylphosphine. *J. Am. Chem. Soc.* **1992**, *114*, 7933. (c) Lu, X.; Zhang, C.; Xu, Z. Reactions of Electron-Deficient Alkynes and Allenes under Phosphine Catalysis. *Acc. Chem. Res.* **2001**, *34*, 535. (d) Sonye, J. P.; Koide, K. Base-catalyzed stereoselective isomerization of electron-deficient propargylic alcohols to E-enones. *J. Org. Chem.* **2006**, *71*, 6254. (e) Kwong, C. K.-W.; Fu, M. Y.; Lam, C. S.-L.; Toy, P. H. The Phosphine-Catalyzed Alkyne to 1,3-Diene Isomerization Reaction.

- Synthesis* **2008**, *15*, 2307 DOI: 10.1055/s-2008-1067173. (f) Pis Diez, C. M.; Fernandez, J. F.; Di Venosa, G.; Casas, S.; Pis Diez, R.; Palermo, J. A. One-step preparation of novel 1-(*N*-indolyl)-1,3-butadienes by base-catalyzed isomerization of alkynes as an access to 5-(*N*-indolyl)-naphthoquinones. *RSC Adv.* **2018**, *8*, 35998.
- (8) Trost, B. M.; Schmidt, T. A simple synthesis of dienones via isomerization of alkyneones effected by palladium catalysts. *J. Am. Chem. Soc.* **1988**, *110*, 2301.
- (9) Selected examples: (a) Ma, D.; Lin, Y.; Lu, X.; Yu, Y. A novel stereoselective synthesis of conjugated dienones. *Tetrahedron Lett.* **1988**, *29*, 1045. (b) Ma, D.; Yu, Y.; Lu, X. Highly stereoselective isomerization of ynones to conjugated dienones catalyzed by transition-metal complexes. *J. Org. Chem.* **1989**, *54*, 1105. (c) Lu, X.; Guo, C.; Ma, D. A Convenient Synthesis of 3-(1,3-Alkadienyl)-2-cycloalken-1-ones. *Synlett* **1990**, *1990*, 357. (d) Guo, C.; Lu, X. Stereoselective synthesis of conjugated polyenones from diyrones. *Tetrahedron Lett.* **1991**, *32*, 7549.
- (10) Kadota, I.; Shibuya, A.; Lutete, L. M.; Yamamoto, Y. Palladium/Benzoic Acid Catalyzed Hydroamination of Alkynes. *J. Org. Chem.* **1999**, *64*, 4570.
- (11) Shintani, R.; Duan, W.-L.; Park, S.; Hayashi, T. Rhodium-catalyzed isomerization of unactivated alkynes to 1,3-dienes. *Chem. Commun.* **2006**, 3646.
- (12) (a) Wang, Z.; Wang, Y.; Zhang, L. Soft Propargylic Deprotonation: Designed Ligand Enables Au-Catalyzed Isomerization of Alkynes to 1,3-Dienes. *J. Am. Chem. Soc.* **2014**, *136*, 8887. (b) Li, X.; Wang, Z.; Ma, X.; Liu, P.-N.; Zhang, L. Designed Bifunctional Phosphine Ligand-Enabled Gold-Catalyzed Isomerizations of Ynamides and Allenamides: Stereoselective and Regioselective Formation of 1-Amido-1,3-dienes. *Org. Lett.* **2017**, *19*, 5744.
- (13) Hirai, K.; Suzuki, H.; Moro-Oka, Y.; Ikawa, T. Catalytic isomerization of acetylenic silyl ethers to dienol silyl ethers by ruthenium hydride complexes. *Tetrahedron Lett.* **1980**, *21*, 3413.
- (14) (a) Cera, G.; Lanzi, M.; Bigi, F.; Maggi, R.; Malacria, M.; Maestri, G. Bi-directional alkyne tandem isomerization via Pd(0)/carboxylic acid joint catalysis: expedient access to 1,3-dienes. *Chem. Commun.* **2018**, *54*, 14021. (b) Cera, G.; Maestri, G. Palladium/Bronsted Acid Catalysis for Hydrofunctionalizations of Alkynes: From Tsuji-Trost Allylations to Stereoselective Methodologies. *ChemCatChem* **2022**, *14*, No. e202200295.
- (15) Selected examples: (a) Shvo, Y.; Blum, Y.; Reshef, D. Rearrangement of 2-butyne-1,4-diol to butyrolactone catalyzed by ruthenium complexes. *J. Organomet. Chem.* **1982**, *238*, C79. (b) Tsuji, Y.; Yokoyama, Y.; Huh, K.-T.; Watanabe, Y. Ruthenium complex-catalyzed *N*-heterocyclization. Syntheses of *N*-substituted pyrroles and pyrrolidines from 1, 4-diols and primary amines. *Bull. Chem. Soc. Jpn.* **1987**, *60*, 3456. (c) Trost, B. M.; Rise, F. Reductive cyclization of 1,6- and 1,7-enynes. *J. Am. Chem. Soc.* **1987**, *109*, 3161. (d) Lu, X.; Ji, J.; Ma, D.; Shen, W. Facile synthesis of 1,4-diketones via palladium complex catalyzed isomerization of alkyne diols. *J. Org. Chem.* **1991**, *56*, 5774. (e) Trost, B. M.; Livingston, R. C. Two-metal catalyst system for redox isomerization of propargyl alcohols to enals and enones. *J. Am. Chem. Soc.* **1995**, *117*, 9586. (f) Kadota, I.; Shibuya, A.; Gyoung, Y. S.; Yamamoto, Y. Palladium/Acetic Acid Catalyzed Allylation of Some Pronucleophiles with Simple Alkynes. *J. Am. Chem. Soc.* **1998**, *120*, 10262. (g) Shi, M.; Wang, B.-Y.; Shao, L.-X. Regioselective control in the palladium-catalyzed isomerization of methylenecyclopropylcarbinols using acetic acid as a reagent. *Synlett* **2007**, *2007*, 0909. (h) Pridmore, S. J.; Slatford, P. A.; Daniel, A.; Whittlesey, M. K.; Williams, J. M. J. Ruthenium-catalyzed conversion of 1,4-alkynediols into pyrroles. *Tetrahedron Lett.* **2007**, *48*, 5115. (i) Tanaka, K.; Shoji, T. Cationic Rhodium(I)/BINAP Complex-Catalyzed Isomerization of Secondary Propargylic Alcohols to α,β -Enones. *Org. Lett.* **2005**, *7*, 3561. (j) Tanaka, K.; Shoji, T.; Hirano, M. Cationic Rhodium(I)/Bisphosphane Complex-Catalyzed Isomerization of Secondary Propargylic Alcohols to α,β -Enones. *Eur. J. Org. Chem.* **2007**, *2007*, 2687. (k) Pridmore, S. J.; Slatford, P. A.; Taylor, J. E.; Whittlesey, M. K.; Williams, J. M. J. Synthesis of furans, pyrroles and pyridazines by a ruthenium-catalyzed isomerisation of alkyne diols and in situ cyclisation. *Tetrahedron* **2009**, *65*, 8981.
- (16) (a) Butler, M. J.; White, A. J. P.; Crimmin, M. R. Isomerization of Cyclooctadiene to Cyclooctyne with a Zinc/Zirconium Heterobimetallic Complex. *Angew. Chem., Int. Ed.* **2016**, *55*, 6951. (b) Butler, M. J.; White, A. J. P.; Crimmin, M. R. Heterobimetallic Rebound: A Mechanism for Diene-to-Alkyne Isomerization with M—Zr Hydride Complexes (M = Al, Zn, and Mg). *Organometallics* **2018**, *37*, 949.
- (17) Kadota, I.; Lutete, L. M.; Shibuya, A.; Yamamoto, Y. Palladium/benzoic acid-catalyzed hydroalkoxylation of alkynes. *Tetrahedron Lett.* **2001**, *42*, 6207.
- (18) (a) Hills, I. D.; Fu, G. C. Elucidating Reactivity Differences in Palladium-Catalyzed Coupling Processes: The Chemistry of Palladium Hydrides. *J. Am. Chem. Soc.* **2004**, *126*, 13178. (b) Gauthier, D.; Lindhardt, A. T.; Olsen, E. P. K.; Overgaard, J.; Skrydstrup, T. In Situ Generated Bulky Palladium Hydride Complexes as Catalysts for the Efficient Isomerization of Olefins. Selective Transformation of Terminal Alkenes to 2-Alkenes. *J. Am. Chem. Soc.* **2010**, *132*, 7998.
- (19) (a) Chen, L.; Ren, P.; Carrow, B. P. Tri(1-Adamantyl)-Phosphine: Expanding the Boundary of Electron-Releasing Character Available to Organophosphorus Compounds. *J. Am. Chem. Soc.* **2016**, *138*, 6392. (b) Chen, L.; Sanchez, D. R.; Zhang, B.; Carrow, B. P. Cationic Suzuki–Miyaura Coupling with Acutely Base-Sensitive Boronic Acids. *J. Am. Chem. Soc.* **2017**, *139*, 12418. (c) Chen, L.; Francis, H.; Carrow, B. P. An “On-Cycle” Precatalyst Enables Room-Temperature Polyfluoroarylation Using Sensitive Boronic Acids. *ACS Catal.* **2018**, *8*, 2989.
- (20) We briefly evaluated the Pd-catalyzed isomerization of a small set of aryl-alkynyl alcohols (1) into dienyl alcohols (2) using C6. See [Supporting Information](#) for details.
- (21) Aside from a parasitic redox process accounting for ca. 14% conversion of **5a**, no isomerization product could be detected.
- (22) For a related discussion on dissociative vs nondissociative chain-walking of alkenes, see the following selected examples: (a) Kochi, T.; Hamasaki, T.; Aoyama, Y.; Kawasaki, J.; Kakiuchi, F. Chain-walking strategy for organic synthesis: catalytic cycloisomerization of 1,*n*-dienes. *J. Am. Chem. Soc.* **2012**, *134*, 16544. (b) Mei, T.-S.; Patel, H. H.; Sigman, M. S. Enantioselective construction of remote quaternary stereocenters. *Nature* **2014**, *508*, 340. (c) Larionov, E.; Lin, L.; Guénee, L.; Mazet, C. Scope and Mechanism in Palladium-Catalyzed Isomerizations of Highly Substituted Allylic, Homoallylic, and Alkenyl Alcohols. *J. Am. Chem. Soc.* **2014**, *136*, 16882. (d) Juliá-Hernández, F.; Moragas, T.; Cornella, J.; Martin, R. Remote carboxylation of halogenated aliphatic hydrocarbons with carbon dioxide. *Nature* **2017**, *545*, 84. (e) Kapat, A.; Sperger, T.; Guven, S.; Schoenebeck, F. *E*-Olefins through intramolecular radical relocation. *Science* **2019**, *363*, 391. (f) Kochi, T.; Kanno, S.; Kakiuchi, F. Nondissociative chain walking as a strategy in catalytic organic synthesis. *Tetrahedron Lett.* **2019**, *60*, 150938.
- (23) (a) Riplinger, C.; Pinski, P.; Becker, U.; Valeev, E. F.; Neese, F. Sparse Maps—A Systematic Infrastructure for Reduced-Scaling Electronic Structure Methods. II. Linear Scaling Domain Based Pair Natural Orbital Coupled Cluster Theory. *J. Chem. Phys.* **2016**, *144*, No. 024109. (b) Weigend, F.; Ahlrichs, R. Balanced Basis Sets of Split Valence, Triple Zeta Valence and Quadruple Zeta Valence Quality for H to Rn: Design and Assessment of Accuracy. *Phys. Chem. Chem. Phys.* **2005**, *7*, 3297. (c) Hellweg, A.; Hättig, C.; Höfener, S.; Klopper, W. Optimized Accurate Auxiliary Basis Sets for RI-MP2 and RI-CC2 Calculations for the Atoms Rb to Rn. *Theor. Chem. Acc.* **2007**, *117*, 587. (d) Weigend, F. Accurate Coulomb-Fitting Basis Sets for H to Rn. *Phys. Chem. Chem. Phys.* **2006**, *8*, 1057. (e) Chai, J.-D.; Head-Gordon, M. Systematic Optimization of Long-Range Corrected Hybrid Density Functionals. *J. Chem. Phys.* **2008**, *128*, 084106. (f) Grimme, S.; Antony, J.; Ehrlich, S.; Krieg, H. A Consistent and Accurate Ab Initio Parametrization of Density Functional Dispersion Correction (DFT-D) for the 94 Elements H–Pu. *J. Chem. Phys.* **2010**, *132*, No. 154104. (g) Grimme, S.; Hansen, A.; Ehlert, S.; Mewes, J.-M. R2SCAN-3c: A “Swiss Army Knife” Composite Electronic-Structure Method. *J. Chem. Phys.* **2021**, *154*, 064103.

(24) Neese, F. Software Update: The ORCA Program System—Version 5.0. *WIREs Comput. Mol. Sci.* **2022**, *12*, No. e1606.

(25) (a) Xu, L.; Hilton, M. J.; Zhang, X.; Norrby, P.-O.; Wu, Y.-D.; Sigman, M. S.; Wiest, O. Mechanism, Reactivity, and Selectivity in Palladium-Catalyzed Redox-Relay Heck Arylations of Alkenyl Alcohols. *J. Am. Chem. Soc.* **2014**, *136*, 1960. (b) Dang, Y.; Qu, S.; Wang, Z.-X.; Wang, X. A Computational Mechanistic Study of an Unprecedented Heck-Type Relay Reaction: Insight into the Origins of Regio- and Enantioselectivities. *J. Am. Chem. Soc.* **2014**, *136*, 986. (c) Ross, S. P.; Rahman, A. A.; Sigman, M. S. Development and Mechanistic Interrogation of Interrupted Chain-Walking in the Enantioselective Relay Heck Reaction. *J. Am. Chem. Soc.* **2020**, *142*, 10516. (d) Cohen, A.; Kaushansky, A.; Marek, I. Mechanistic Insights on the Selectivity of the Tandem Heck Ring-Opening of Cyclopropylidol Derivatives. *JACS Au* **2022**, *2*, 687.

(26) (a) Bursch, M.; Mewes, J.; Hansen, A.; Grimme, S. Best-Practice DFT Protocols for Basic Molecular Computational Chemistry. *Angew. Chem., Int. Ed.* **2022**, *61*, No. e202205735, DOI: [10.1002/anie.202205735](https://doi.org/10.1002/anie.202205735). (b) Eisenstein, O.; Ujaque, G.; Lledós, A. What Makes a Good (Computed) Energy Profile?. In *New Directions in the Modeling of Organometallic Reactions*; Lledós, A.; Ujaque, G., Eds.; Springer International Publishing: Cham, 2020; Vol. 67, pp 1–38. (c) Norjmaa, G.; Ujaque, G.; Lledós, A. Beyond Continuum Solvent Models in Computational Homogeneous Catalysis. *Top. Catal.* **2022**, *65*, 118.

(27) At 80 °C, 1.53 kcal/mol difference would correspond to a ratio of 8.8:1 between **5a** and **3a**.